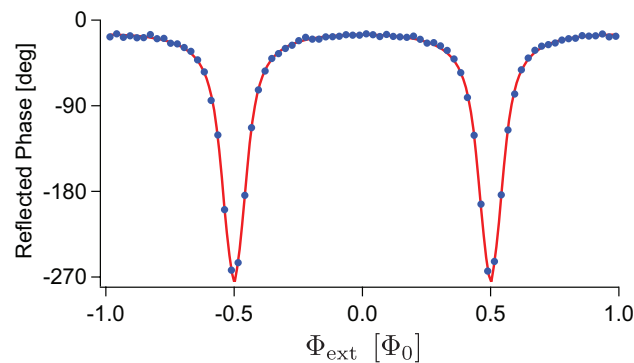
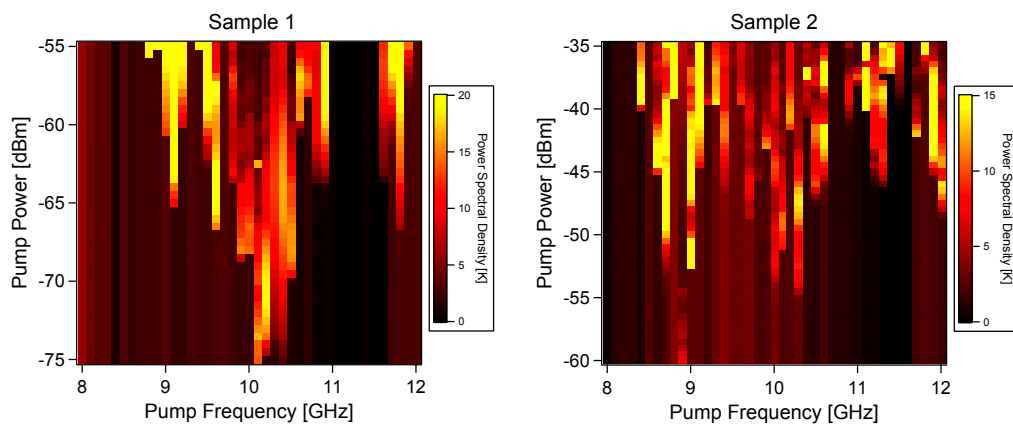


Supplementary Information

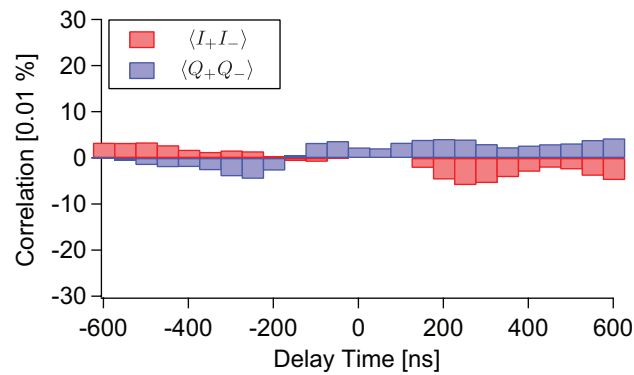
Supplementary Figures



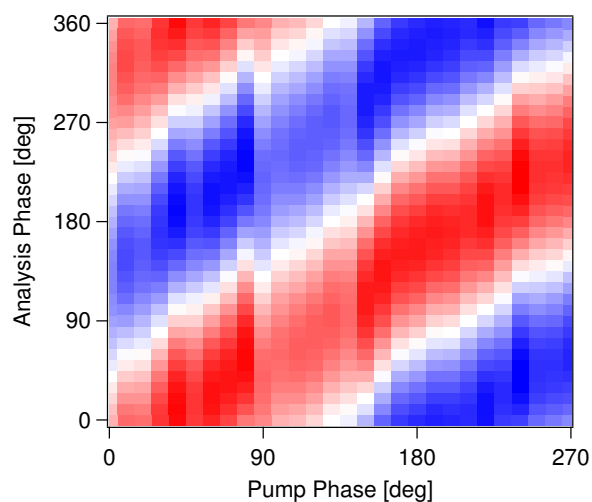
Supplementary Figure 1: Modulating the effective length of the line. As a basic characterization, we can measure the phase shift of a microwave probe signal reflected from the SQUID as we change Φ_{ext} . This illustrates how the SQUID changes the boundary condition at the end of the line. The data is for sample 1, measured with a 5 GHz probe. The fit includes the SQUID capacitance which is important near $\Phi_{\text{ext}} = \pm 0.5\Phi_0$. From the fit, we extract a plasma (self-resonance) frequency of 85 GHz, although there is a systematic uncertainty in this value due to the unknown SQUID asymmetry.



Supplementary Figure 2: Photons generated by the dynamical Casimir effect. Here we show the output power of the transmission line while driving the SQUID. On the left (right), are the results for sample 1 (2). We scan the pump power and frequency and look at the power emitted into the CPW. The analysis frequency tracks the drive at $f_d/2$, which we expect to be the center frequency of the DCE radiation. We clearly see photon generation for essentially all drive frequencies spanning the 8-12 GHz band set by the filtering of the line. This corresponds to an analysis band of 4-6 GHz.



Supplementary Figure 3: Parasitic cross correlation of the amplifier noise. The cross-correlation function measured with the pump off, showing the parasitic correlation of the amplifier, measured under the same conditions as Fig. 3a. Note that the vertical scale is expanded by a factor of 100 compared to Fig. 3a. We see that any parasitic correlation of the amplifier is negligible.



Supplementary Figure 4: The effects of phase rotations on the correlations. In a two-mode squeezed state, we expect that the various quadrature cross-correlation functions are related to each other by phase rotations. To explore this predicted symmetry, we can compute the complex correlation function Ψ (defined in the supplementary methods) from the measured correlation functions and study its rotation properties. The color scale is the real part of Ψ . The x -axis corresponds to a change in the drive phase. The y -axis corresponds to a digital rotation of the measured value of Ψ . As expected for TMS, we see that Ψ is symmetric under phase rotations, that is, the rotation of one phase cancels a rotation of the other.

Supplementary Discussion

We can consider if some spurious effect unrelated to the DCE is the source of the observed photon flux. Simple heating or mixing down of high frequency noise is strongly ruled out by the symmetry of the spectrum and the observed TMS which singles out $f_d/2$ as a special frequency and strongly indicate a two-photon process. A nonlinearity in the dielectric response of the substrate could also conceivably lead to parametric downconversion. However, the nominal pump powers used correspond to electric fields of less than 10 V/m, many orders of magnitude below the levels where nonlinear effects would be expected. We can also consider spurious effects related to the SQUID. For an ideal SQUID, the circulating current mode, which we pump, and the linear current mode, which is coupled to the output line, are not coupled. However, an asymmetry in the junction areas will produce a cross coupling. The first order effect of this is simply to inject a coherent current into the output line at the drive frequency.¹⁶ We could imagine that if this injected current is large, then it could lead to parametric downconversion due to the electronic nonlinearity of the SQUID. We have directly measured the parasitic cross-coupling between the pump and output lines, and find that the isolation is better than 50 dB, implying that the power injected into the output line is less than 1 fW. Again, this is many orders of magnitude below the level of power needed for parametric downconversion, and, in fact, more than an order of magnitude smaller than the total observed output power. Furthermore, a current injected in the SQUID at f_d will actually modulate the SQUID inductance at $2f_d$, leading to downconversion symmetric around f_d and not $f_d/2$ as we observe.

Supplementary Methods

Theoretically, we treat the problem as a scattering problem in the context of quantum network theory.²⁶ For superconducting circuits, it is convenient to describe the EM field in the transmission line in terms of the phase field operator $\phi(x, t) = \int_{-\infty}^t E(x, t') dt'$, where $E(x, t)$ is the electric field operator. In the transmission line, $\phi(x, t)$ is described by the massless, scalar Klein-Gordon equation in one dimension, the solution of which can be written as $\phi(x, t) = \phi_{\text{in}}(x - c_0 t) + \phi_{\text{out}}(x + c_0 t)$, where $\phi_{\text{in(out)}}$ is the field propagating inward to (outward from) the SQUID and $c_0 \sim 0.4c$ is the speed of light in the transmission line. We solve the scattering problem in Fourier space defining

$$\phi_{\text{in(out)}} = \sqrt{\frac{\hbar Z_0}{4\pi}} \int_0^\infty \frac{d\omega}{\sqrt{\omega}} \left(a_{\text{in(out)}}(\omega) e^{-i(\mp k_\omega x + \omega t)} + h.c. \right)$$

where $a(\omega)$ and its hermitian conjugate $a^\dagger(\omega)$ are the standard annihilation and creation operators and $k_\omega = \omega/c_0$ is the wavenumber of the radiation. Solving the scattering problem then amounts to finding expressions for $a_{\text{out}}^\dagger(\omega)$ and $a_{\text{out}}(\omega)$ as a function of $a_{\text{in}}^\dagger(\omega)$ and $a_{\text{in}}(\omega)$. The boundary condition imposed by the SQUID determines the connection between these operators. With the output operators, we can then calculate the properties of the measurable output field assuming the input field is in a definite state, such as a thermal state or vacuum state. For a static magnetic flux, Φ_{ext} , we obtain the simple expressions $a_{\text{out}}(\omega) = R(\omega)a_{\text{in}}(\omega)$ where $R(\omega)$ is the reflection coefficient from the SQUID. $R(\omega) = -\exp[2ik_\omega\ell_e(\Phi_{\text{ext}})]$ has the simple form¹⁶ of a phase shift due to a transmission line of fixed length $\ell_e(\Phi_{\text{ext}}) = L_J(\Phi_{\text{ext}})/L_0$. Here $c_0 = 1/\sqrt{L_0C_0}$, L_0 (C_0) is the inductance (capacitance) per unit length of the line, $L_J(\Phi_{\text{ext}}) = (\Phi_0/2\pi)^2/E_J(\Phi_{\text{ext}})$ is the Josephson inductance of the SQUID, E_J is its Josephson energy, and $\Phi_0 = h/2e$ is the superconducting flux quantum.

In order to generate DCE radiation, ℓ_e must change with a nonuniform acceleration. A simple example of this type of motion is a sinusoidal drive with an amplitude of $\delta\ell_e$. If it is driven at ω_d with a small amplitude, we then find the simple expression¹⁷ for $a_{\text{out}}(\omega)$ in the region $\omega < \omega_d$:

$$a_{\text{out}}(\omega) = R(\omega)a_{\text{in}}(\omega) + S(\omega)a_{\text{in}}^\dagger(\omega_d - \omega)$$

where $S(\omega) = -i(\delta\ell_e/c_0)\sqrt{\omega(\omega_d - \omega)}A(\omega)A^*(\omega_d - \omega)$ and $A(\omega)$ is the spectral amplitude of the transmission line. Crucially, the time-dependent boundary leads to mixing of the input field's creation and annihilation operators. With this expression we can calculate the output photon flux density for an input thermal state

$$n_{\text{out}}(\omega) = \langle a_{\text{out}}^\dagger(\omega)a_{\text{out}}(\omega) \rangle = n_{\text{in}}(\omega) + |S(\omega)|^2n_{\text{in}}(\omega_d - \omega) + |S(\omega)|^2.$$

The first two terms, proportional to $n_{\text{in}}(\omega)$, represent the purely classical effects of reflection and upconversion of the input field to the drive frequency. They are zero at zero temperature. The last term is due to vacuum fluctuations and is, in fact, the DCE radiation.

Theory¹⁷ also predicts that the output should exhibit voltage-voltage correlations at different frequencies with a particular structure commonly known as two-mode squeezing (TMS). Following Ref. 25, we can describe a two-photon state, as we expect the DCE to generate, in terms of a modulation of the center frequency of the state. We can then define the modulation operators as $\alpha_1(\epsilon) = [\lambda_+a(\omega_+) + \lambda_-a^\dagger(\omega_-)]/\sqrt{2}$ and $\alpha_2(\epsilon) = [-i\lambda_+a(\omega_+) + i\lambda_-a^\dagger(\omega_-)]/\sqrt{2}$, where $\omega_\pm = \omega_d(1 \pm \epsilon)/2$ and $\lambda_\pm = (1 \pm \epsilon)^{1/2}$. The factors λ_\pm rescale the operators from quanta at ω_\pm to quanta at the center frequency $\omega_d/2$. We see that these operators mix excitations at the upper and lower sidebands of the field with a

definite phase. The TMS of the field then appears as an imbalance of the noise in one of these modes compared to the other. We define the normalized TMS

$$\sigma_2 = \frac{\Sigma_{11} - \Sigma_{22}}{\Sigma_{11} + \Sigma_{22}}$$

where $\Sigma_{mn} = \langle \alpha_m \alpha_n^\dagger + \alpha_n^\dagger \alpha_m \rangle / 2$ is the symmetrized spectral density matrix. We can then calculate the TMS of the output field to be

$$\sigma_2 = \frac{D(\epsilon)v_e}{2c_0} \frac{(1 - \epsilon^2)}{1 + (D(\epsilon)v_e/2c_0)^2(1 - \epsilon^2)}.$$

This predicts a maximum squeezing of 50%.

Experimentally, we measure the four quadrature voltages of the upper and lower sidebands I_\pm and Q_\pm . The observable (hermitian) quadrature operators can be related to creation and annihilation operators as

$$I_\pm = \sqrt{\frac{\hbar\omega_\pm Z_0}{8\pi}} [a(\omega_\pm) + a(\omega_\pm)^\dagger] \quad ; \quad Q_\pm = -i\sqrt{\frac{\hbar\omega_\pm Z_0}{8\pi}} [a(\omega_\pm) - a(\omega_\pm)^\dagger].$$

We can write σ_2 in terms of the quadratures as

$$\sigma_2 = \frac{1}{P_{\text{avg}}} (\langle I_+ I_- \rangle - \langle Q_+ Q_- \rangle)$$

where $P_{\text{avg}} = (\langle I_+^2 \rangle + \langle Q_+^2 \rangle + \langle I_-^2 \rangle + \langle Q_-^2 \rangle) / 2$ is the average noise power in the sidebands. We also expect a special structure for the correlations, in particular that $\langle I_+ I_- \rangle = -\langle Q_+ Q_- \rangle$ and that $\langle I_+ Q_- \rangle = \langle I_- Q_+ \rangle$. Finally, we comment that by the proper choice of analysis phase, we can specify $\langle I_+ Q_- \rangle = \langle I_- Q_+ \rangle = 0$ without loss of generality, which has been done in writing the above equation.

We can also predict how the correlations transform under rotations of the phase of the EM field by an angle θ . In particular, if we define the appropriate combination of correlation functions

$$\Psi = (\langle I_+ I_- \rangle - \langle Q_+ Q_- \rangle) + i(\langle I_+ Q_- \rangle + \langle I_- Q_+ \rangle)$$

we expect Ψ to transform such that $\Psi' = e^{-2i\theta}\Psi$. To explore this predicted symmetry, we can compute the complex quantity Ψ from the experimental correlation functions and look at the rotation properties (see Sup. Fig. 4).

Two-mode squeezing is often discussed in terms of the unitary squeezing operator $\Theta(r) = \exp[ra(\omega_+)a(\omega_-) - ra^\dagger(\omega_+)a^\dagger(\omega_-)]$ where r is called the squeezing parameter. To connect to this language, one can show that $\sigma_2 = -\lambda_+ \lambda_- \tanh(2r)$. This then gives $r = (\delta\ell_e/c_0)\sqrt{\omega_+\omega_-}$.

In Fig. 3a and Sup. Fig. 3, we have displayed time correlation functions (TCF) which are the Fourier transforms of the frequency correlation functions (FCF) defined above. In particular, the value of the TCF at zero delay is the integral of the FCF in the measurement bandwidth. If we assume that the FCF is approximately constant in the measurement bandwidth, the integral reduces to multiplying the FCF by a constant factor. This is the same for all the TCF, and therefore cancels out of the normalized quantities displayed.